The past climate of the Indian region as seen from the modelling world

Charan Teja Tejavath[1,*], Pankaj Upadhyay[1,2] and Karumuri Ashok[1]

[1]Centre for Earth, Ocean and Atmospheric Sciences, University of Hyderabad, Hyderabad 500 046, India
[2]Present address: Centre for Atmospheric Sciences, Indian Institute of Technology, New Delhi 110 016, India

Proxy-reconstruction studies suggest several waxing and waning epochs of the Indian summer monsoon (ISM) since Last Glacial Maximum (LGM; ≃21 kyr BP). These fluctuations in the ISM are attributed to several internal and external factors. The few available past climate modelling studies for various epochs also support the results from the reconstruction studies for India. Our results, based on an analysis of five CMIP5-PMIP3 simulations for the periods of LGM, Mid-Holocene (MH; ≃6 kyr BP), last-millennium and historical period (CE 1901–1999) indicate that the ISM rainfall was lowest during the LGM, and strongest during the MH. The simulations, relative to the historical time period, suggest highest low-level convergence over the Indian region during MH and lowest during LGM. These slow changes in large-scale circulation patterns resulted in relatively highest simulated ISM rainfall during the MH, and lowest in the LGM.

Keywords: Indian summer monsoon, Last Glacial Minimum, Mid-Holocene, Last Millennium, past climate modelling, PMIP3 simulations.

Introduction

THE Indian monsoon system is a complex, large-scale system comprising distinct seasonal circulation features and precipitation patterns. Any changes in the normal seasonal rainfall or occurrence of extreme events, such as droughts and floods, etc., disrupt the livelihood of 1.5 billion people, economy and agriculture of India[1–6]. The area-averaged Indian summer monsoon rainfall, occurring over the months of June–September, is estimated to be 890 mm (ref. 7). Guhathakurta and Rajeevan[8] using the India Meteorological Department (IMD) ground-based observational data for the period 1901–2000 show ISMR is stable and has not shown any noticeable overall trend, but the extreme events are suggested to have increased[9]. However, studies demonstrate a weakening of the summer monsoon rainfall in several states[10,11]. Sanap *et al.*[12] and Krishnan *et al.*[13] attribute the weakening of monsoon circulation to a warming climate. Roxy *et al.*[14] show a decreasing trend in ISMR over the central-east northern regions of the Indian subcontinent, and south of the Western Ghats region using the IMD and CRU observed rainfall datasets from 1901 to 2012. Further, the maximum surface temperatures for the pre-monsoon months (April and May) over India show a multi-decadal increase during the 1950–2010 period[15].

There are numerous studies on the interannual variability (IAV) of ISM, which use the modern instrumental data for the Indian region[16–18]. The earliest research on interannual variations of the Indian monsoon led to the eventual discovery of two important climatic drivers, the El Niño-Southern Oscillation (ENSO)[19] and Himalayan/Eurasian snow cover (ESC)[20]; these drivers are important for the interannual variability (IAV) of Indian summer monsoon (ISM). The ENSO phases of El Niño and La Niña are commonly linked to the failure and strengthening of ISM respectively. Kumar *et al.*[21] suggested that ENSO–ISM teleconnections are weakening in the late 1990s, particularly 1997, a year of a major El Niño. They suggested that this weakening was owing to an increased anthropogenic warming. Various other reasons such as the frequent occurrence of Indian Ocean Dipole (IOD)[22–26] events, decadal variations in monsoon[27], varying phases of the Pacific decadal oscillation that affect the interannual teleconnections of ENSO[28–31] have also been suggested. There is another argument that this weakening of ENSO–monsoon relationship may be due to statistical sampling[31,32]. Further details can be found in refs 33, 34.

Notably, instrumental records of past climate data are practically non-existent prior to the CE 1850s. The last ~100–150 years are the best documented period in terms of instrumental observations. However, uncertainties exist in terms of the spatial coverage and quality of the data even for this period.

Understanding the past and present climate variability of ISM will be indispensable for determining its future of variability, and even ascertaining that the current changes in observed relationships, such as the ISM–ENSO do not necessarily arise out of sampling issues, and to understand the mechanisms better. In this context, it is highly desirable to collect and examine any datasets on the past climate variability of the Indian region, particularly during the mid-Holocene period when the ENSO–monsoon–IOD associations have been reflected in the proxy datasets[35].

*For correspondence. (e-mail: charan0239@gmail.com)

To this end, proxy data collection analysis, and model simulations are useful. Unfortunately, the proxy sample collection is a laborious and expensive business. Consequently, only a few studies are carried out, and redundant studies for verification are relatively rare, particularly for the Indian summer monsoon region. In this context, modelling studies, notwithstanding the limitations of reproduction, provide a complementary tool. For example, an analysis of multi-model simulations of the Palaeoclimate Modelling Intercomparison Project 3 (PMIP3) and Coupled Model Intercomparison Project 5 (CMIP5) vintage[36,37] show a multi-centennial variation in the ENSO–monsoon links associated with changes in the background Walker circulation in the tropical Indo-pacific, and similar slow changes in the moisture availability[37].

In this article, we briefly review the available modelling studies of the Indian summer monsoon for the LGM and Holocene periods, and discuss them in light of available proxy studies. We then present results from our analysis of CMIP5/PMIP3 simulation outputs for the period spanning from the LGM through the present day (CE 1901–1999), with a focus on the mid-Holocene period, when the ENSO variance is suggested to be relatively weak[38].

Indian summer monsoons during LGM through mid-Holocene

Proxy-data based studies

The LGM and Younger Dryas periods: Chabangborn *et al.*[39] using both modelling and reconstructed palaeo-data showed a weak ISM associated with dry climatic conditions during LGM, in agreement with Patnaik *et al.*[7]. Chabangborn *et al.*[39] suggest that a very diverse ITCZ position during the LGM compared to the current period may be the potential reason for the weakening of ISM during LGM from both modelled and reconstructed data. During the late Pleistocene to Holocene transition, the ISM has witnessed abrupt changes[40,41]. Also, during the Younger Dryas period (i.e. 11.7 kyr BP to 11.1 kyr BP), a rather weak ISM has been observed[40,41]. The weakened ISM is suggested to be associated with the Atlantic Meridional Overturning Circulation which caused a change in the meridional thermal gradient in the Indian region, and the consequent southward shift in the mean latitudinal position of ITCZ relative to the current day[41]. Furthermore, a multi-proxy study based on an analysis of lake sediment reconstructions from peninsular India[42] shows that during the Younger Dryas period, the ISM was weaker over the southern part of India.

The Holocene: The Holocene period has been known for its abrupt changes in the solar forcing[43]. Interestingly, the consequent climate variability within the period has even been claimed to have resulted in several disruptions of human civilization[44]. To be sure, the few available proxy-based past climate records from the Indian subcontinent and the Arabian sea show centennial to millennial timescale variability in the ISMR during the Holocene[45–50]. These studies, in general, show a long-term weakening trend in ISMR from the early Holocene (9 kyr BP) to late Holocene (3 kyr BP). Ali *et al.*[41] and Sandeep *et al.*[42] also suggest that a strong and stable ISM during 10.6 kyr BP to 8 kyr BP is followed by a gradual decline during 8 kyr BP to 3 kyr BP with a few punctuations in between periods. Notably, another proxy-based study[51], which uses reconstructed monsoon rainfall anomalies over India, multiple SST reconstructions from west to east equatorial Pacific, and reconstructed summer wind-stress curl datasets off the coastlines of Arabian Sea, shows that rainfall in northwest India during 10 kyr BP was higher than that for the current day by 40–60%, and in general high also in the core ISM region. On the contrary, the concurrent rainfall over northeast India is shown to be lesser than that for the current day by 10–30% and to have weakened throughout from the mid to late Holocene. Importantly, Gill *et al.*[51] suggest that, from early to mid-Holocene, La Niña like tropical Pacific teleconnections played a dominant role in enhancing the ISM. Prasad *et al.*[52], based on a sediment core from Lonar Lake in Central India, suggest an early Holocene onset of intensified monsoon in the region, which they claim is similar to that reported from other ISM proxy records, and occurrence of prolonged droughts in the region between 4.6 kyr BP to 3.9 kyr BP and 2 kyr BP to 0.6 kyr BP. Prasad *et al.*[52] suggest a long-term influence of ENSO-like conditions on ISM, and also that Southern Indo-Pacific warm pool (IPWP) and ISM links vary, affecting the multi-centennial large scale transport of advection of moist air towards India.

Various other, or linked, mechanisms have also been proposed for the Holocene variations of the ISM based on proxy data analysis. Fleitmann *et al.*[46], for example, using stalagmites from Oman and Yemen, and comparing their findings with earlier studies, suggest that during the early Holocene (10.5 kyr BP to 9.5 kyr BP), the mean summer latitudinal position of ITCZ apparently advanced swiftly northward beyond its mean current position (see figure 5 of Fleitmann *et al.*[46]), increasing the monsoonal rainfall. However, in response to the solar insolation changes, the mean latitudinal position of ITCZ is indicated to have continuously moved to southward from 7.8 kyr BP to the present, thereby weakening the ISM intensity and precipitation[46]. Importantly, they conjecture that there was no weakening of the ISM intensity during 5 kyr BP to 4 kyr BP. Furthermore, Dixit *et al.*[53] using the lake sediments show that solar insolation played a crucial role in ISM having its 'greatest' strength between 9.4 kyr BP to 8.3 kyr BP, the early Holocene period. The result is supported by other proxy studies[42,54–56]. Following its greatest strength between 8.3 and 7.9 kyr BP, the ISM

faced a sudden weakening which coincided with the 8.2 kyr BP abrupt event. Interestingly, Dixit *et al.*[53] and Band *et al.*[56] propose that the abrupt weakening of ISM around 8.2 kyr BP is caused by the 'North Atlantic cold event' due to a slowdown of Atlantic meridional overturning circulation.

Band *et al.*[56], based on analysis of the stalagmite oxygen isotope ratios from the Kotumsar cave in central India, suggest that, with decreasing insolation, the summer monsoon rainfall in central India may have started declining at the beginning of the mid-Holocene from 8.5 kyr BP to 6.5 kyr BP, in apparent agreement with previous ISM reconstructions with coarser resolutions, but only to gradually increase from 6.5 kyr BP to 5.6 kyr BP. Jalihal *et al.*[57] identify the solar insolation as a trigger for precipitation changes on orbital timescales, but suggest that vertical stability and surface energy are also important. Apart from the insolation changes, potentially changing north Atlantic teleconnections, as well as increased frequency in the ENSO events, also may have played crucial roles in ISM variability during MH[56]. A proxy-observational study[58] suggests that the prevalence of strengthened mid-latitude westerlies, and an overall weakening of the ISM during the mid to late Holocene period, may have had implications for the Himalayan glaciers; however, fluctuating climatic conditions were observed during this period.

Several studies have focused on a specific sub-period or 'significant climate episodes' of the Holocene. Proxy studies[59–61] suggest that a sudden weakening of the ISM intensity during 4.2 kyr BP may have triggered the end of Indus valley civilization. Berkelhammer *et al.*[62], using a speleothem stable isotope record from northeast India, find an abrupt Holocene climatic change event at around 4 kyr BP, a period now identified as the Meghalayan by the International Commission on Stratigraphy (https://www.geologyglasgow.org.uk/news/article/the-meghalayan-age--a-new-unit-of-the-geologic-time-scale/). A contemporary study[63], based on fluvial morphodynamics studies and after chronological analysis of fluvial and aeolian deposits, etc., from the Sindh region in Pakistan, also suggests a weakening of the monsoon approximately 3900 years ago. According to Ali *et al.*[41], the ISM stabilization took place earlier, at around 3 kyr BP, with enhanced ISM during 2.8 kyr BP, 2.1 kyr BP, and later, the medieval warm period. Interestingly, Rawat *et al.*[64] report that the ISM strengthened from 6.7 kyr BP to 3.3 kyr BP, which contradicts Ali *et al.*[41]. Sinha *et al.*[65] show that the abrupt changes in the ISM during 2.8 kyr BP coincide with the North Atlantic cold event linked with the low solar activity during that period. Sandeep *et al.*[42] suggest that a steady ISM is observed from 3 kyr BP to present.

As the ENSO is one of the major ISM drivers, we shall briefly list the relevant papers here. Gill *et al.*[66] based on multiple proxy reconstructions show enhanced La Niña conditions during 10 kyr BP commensurate with the concurrent higher ISMR, and a gradually warmer eastern equatorial Pacific till 2 kyr BP. Interestingly, proxy studies by several other researchers indicate a 'suppressed' ENSO activity during MH[35,67–69], which is corroborated by the PMIP2 model simulations[38]. It must, however, be noted that an analysis of the PMIP3 models in the same study suggests such simulated suppressed activity to be marginal. This suppressed ENSO activity is attributed to the weakened air–sea interactions with reduced precipitation and basin-wide cooling activity[38]. On the other hand, model experiments[70] suggest that the (El Niño) activity during 8 kyr BP is due to changes in Asian monsoon, which in turn is controlled by solar insolation changes.

The last millennium: A recent review by Dixit and Tandon[71] based on multiple proxy records, shows heterogeneity in terms of region and time for the most prominent climate optimums during the Last Millennium (LM), known as Medieval Warm Period (MWP) and Little Ice Age (LIA). Cook *et al.*[72], using the Monsoon Asia Drought Atlas (MADA), which has been prepared using 327 tree-ring chronologies with self-calibrating Palmer Drought Severity Index (PDSI) method for CE 1300–2005 period, suggest that most parts of India, particularly the western part, suffered wide-spread and persistent mega-droughts during LM; but the periods and longevity of the droughts varied across the region. Cook *et al.*[72] claim that the four major Asian mega droughts of the LM coincide with the LIA period. Rehfeld *et al.*[73], using several independent proxy datasets across Asia, including eleven samples from Indian region, suggest a warmer and wetter ISM during the MWP, and a relatively cooler and drier ISM during the LIA. Interestingly, few other proxy-based studies also suggest that ISM was stronger[74,75] and wetter[76,77] during MWP. On the other hand, Ali *et al.*[41] and Sanwal *et al.*[76] report that ISM was stronger and wetter in the condition during LIA. As can be understood, some of the contradictions of the conditions in the LIA may be due to the location where the sample has been obtained, and the type of the proxy.

Rehfeld *et al.*[73] hypothesize that an earlier retreat of the Tibetan High facilitates an earlier onset of the summer monsoon, leading to a longer seasonal cycle, and consequently a warm and wet ISM during the MWP. Polanski *et al.*[77,78], in a modelling and proxy analysis, report that solar insolation played a major role in weakening and enhancement of summer and winter Indian monsoon rainfall, but interestingly, through colder and warmer Indian Ocean SST patterns. Cook *et al.*[72] suggest that Asian mega droughts, which were referred to in the earlier paragraph, were associated with El Niño events. Ummenhofer *et al.*[79] using both MADA and reconstructed PDSI data also show that the droughts in South Asia are mostly coincident with co-occurring El Niño and IOD events or only El Niños, while independent IOD events are coincident with a significantly enhanced South Asian monsoon.

Apart from the above, Chakraborty *et al.*[80] using coral oxygen isotopic records from the equatorial Pacific ocean show that tropospheric temperature (TT) gradient related to ENSO[9], played a major role in driving the climate variability of ISM during the LM. Sinha *et al.*[81] suggest that on longer time scales, e.g. millennial time scale, thermodynamic effect, and changes in land conditions have been important for monsoonal variations; on shorter time scales, the ISM variability is more strongly influenced by the local and remote SST patterns and external boundary conditions.

Relevant modelling studies

Most of the palaeo-modelling studies relevant to Indian climate are for the mid-Holocene and last millennium. A coupled model study[82], shows that summer insolation played a major role in observed enhancement in south Asian monsoon during the early Holocene, but the ocean feedback was in turn opposite. Model studies[83–87] suggest that the northern hemisphere monsoons, including the Indian monsoon, exhibited the enhancement due to insolation changes through the direct radiative forcing. A multi-model analysis[88] shows insolation changes during the mid-Holocene affected the ISM retreat through the dipole patterns in the late summer northwest Indian Ocean sea surface temperatures.

A study using both proxy datasets and the CSIRO model simulations under the aegis of PMIP3 protocols[89] suggests that the area-averaged mean annual precipitation cycle over India did not change in MH, LM and HS periods. They suggest, however, a change in spatial patterns associated with a lateral shift in ITCZ, and a weakened summer monsoon rainfall in MH – a result that is different from the results from various other proxy studies[57,65]. Importantly, the suggestion of the shift in the ITCZ by Kumar *et al.*[89] is subject to the interpretation of a pattern of June–September OLR, connecting a peak in the southwest region of Kerala with another peak in the above the northeast region (see figure 6 *a* of Kumar *et al.*[89]), i.e. somewhat resembling as a mirror image of the letter *Z*, as the ITCZ. However, the large-scale rainfall over the Indian monsoon zone during the summer monsoon season, extending from southeast of Pakistan into the Head Bay of Bengal, is referred to as the continental ITCZ (CTCZ) to distinguish it from the more common ITCZ seen over the tropical oceans[90]. Therefore, it would still be important to explore whether Holocene rainfall changes are associated with the changes in CTCZ or the tropical (~5°N) ITCZ – or both of them. Importantly, Kumar *et al.*[89] also suggest that the Himalayan region had received relatively higher monsoonal rainfall during the late Holocene because of 850 hPa westerlies. Polanski *et al.*[91] using both multiple proxy-reconstruction data and atmospheric regional model show that the monsoon intensity was influenced by changes report in solar radiation during MH. According to them, a weakening of the monsoonal winds, and a southward of the same caused more summer monsoon rainfall over the southern part of India as well as windward slopes of portions of western and southern Himalayas, but reduced summer monsoon rainfall over the central part of Indian and Bay of Bengal regions.

A 1000-year control simulation employed by a single model (MRI-CGCM2.2)[92] shows a robust ENSO–ISM relationship. A modelling study using CMIP5/PMIP3 simulations[93] shows that Asian mega droughts during the last millennium are mostly linked with the El Niño-events. Tejavath *et al.*[36,37] used the available CMIP5/PMIP3 simulations and report that a majority of the nine models in the study simulate wetter and drier ISM conditions during the MWP and LIA respectively relative to the LM-mean, are in agreement with the earlier studies[41,73,77,94]. Further, the ENSO is significantly correlated with the area-averaged ISM rainfall during both MWP and LIA of the LM in the PMIP3 simulations by all these models[36,37]. The study also suggests that there is a nonlinearity in the ENSO–ISM association from MWP to LIA, leading to an enhanced ISMR during MWP and deficit ISMR during LIA; this is apparently associated with a multi-centennial background change in the zonal circulation and increased availability of moisture during the warmer MWP[37]. Indeed, proxy data-based studies[46,74] claim that the ISM response to the changes in the solar insolation from the last 20 kyr BP is not necessarily linear. Further, Carre *et al.*[95] conclude in their proxy-based study that ENSO sensitivity is not only limited to the changes in insolation. Studies[96,97] show that solar and/or volcanic forcings, coupled with ocean–atmosphere feedbacks, explain the LIA cooling trend. Rehfeld and Laepple[98] show that the climate model outputs only provide large scale trends based on the first order effects of CO_2 and orbital forcing.

Studies[77,78] based on both proxy data analysis and atmospheric modelling conclude that multi-decadal variations have been more prominent during both MWP and LIA relative to the present day climate. Furthermore, they suggest that driving mechanisms for dry summer monsoon periods during both MWP and LIA are similar to those for the present day climate. They also show, during the MWP, that the strongest convection activity happened over the Arabian Sea and India, whereas during the LIA these regions received less rainfall. These rainfall changes are attributed to the shift in regional atmospheric circulation patterns driven by Indian Ocean SST anomalies. These SST anomalies, in turn, are indicated due to changes in external forcings like solar insolation, and internal forcing and feedback from the surrounding oceans[77]. The authors also suggest that the northern Arabian Sea SST patterns influence the moisture anomalies of the Central Indian region[77]. Further, reconstructed and simulated annual moisture signals for Central India are in agreement with signals over the Himalaya[77] during the LM. The study also suggests that while extra-tropical

westerlies during winter influenced western and central Himalayas, the eastern Himalayan region during the summer is affected by changes in the land–sea thermal gradient, and a strengthened ISM-east Asian summer monsoon link. However, nine coupled simulations from the PMIP3 do not exhibit any statistically significant association of the ISMR during the MWP and LIA periods with the meridional land–sea gradient spanning the Indian subcontinent[37].

Interestingly, the concentrations of the greenhouse gases during the early Holocene are not different from the last millennium period[71], except for, as can be conjectured, probably the recent 175 years are so[70]. However, the solar forcing was different. As discussed above, the multi-model simulations from CMIP5/PMIP3 model studies have been able to capture the broad trends in the rainfall and temperature during the ISM season coherently throughout the LM.

The PMIP3 multi-model simulations provide a measure of inter-model spread. For example, among the feedbacks such as shortwave cloud and vegetation feedbacks across the PMIP3 LGM and MH simulations, the shortwave cloud feedback is suggested to be a major contributor for the inter-model uncertainties[99]. Also, the drift in most models is directly attributed to a large amount of heating by solar radiation in high and middle latitudes[100]. Notwithstanding this, even a qualitative agreement across models about any climate statistic indicates its validity, or a plausibility of the occurrence of an associated climate phenomenon in the real world, as the case may be. Therefore, we carry out an analysis of the simulated mean ISM from these datasets.

Data and methodology

In this study, we use simulations, by five models, from the CMIP5/PMIP3 (refs 101, 102), whose climate simulations were available for at least 100 year time slices for the last glacial maximum period (21 kyr BP), mid Holocene (6 kyr BP), last millennium (CE 0850–1850) and historical period (CE 1901–1999), to study the IAV of ISM during the past climate. The five models namely, Community CSM4 (CCSM4), IPSL-CM5A-LR (IPSL), MRI-CGCM3 (MRI), GISS-E2-R (GISS) and MPI-ESM-P (MPI) have been selected based on the above criteria. We use a total of five available time-slice simulations of past climate epochs, each lasting 100 years, pertaining to each of the above mentioned models. These epochs are Last Glacial Maximum simulations (LGM; 21 kyr BP), mid Holocene simulations (MH; 6 kyr BP), Medieval Warm Period (MWP; 1 kyr BP), Little Ice Age (LIA; 0.45 kyr BP and Historical period simulations (HS; CE 1901–1999), which correspond to the recent period. The MWP & LIA are part of the longer last millennium simulations[37,102]. Following Tejavath *et al.*[37], we designate the relatively warmest (coldest) 200 year period of the last millennium simulations as the simulated MWP (LIA) period for maintaining uniformity between global and regional analysis of ENSO–ISM teleconnections from the PMIP3 LM simulations, with the knowledge that the temporal and spatial signatures of the MWP and LIA varied from region to region, at least in terms of magnitude[71,103]. The extent of MWP & LIA periods in the models are respectively, CE 1000–1199 and CE 1550–1749, broadly commensurate with the respective periods of CE 950–1350 and CE 1500–1850 from the proxy studies[35,104–107].

As can be conjectured, it would be a difficult task to validate the CMIP5/PMIP3 past climate simulations for the LGM, MH, MWP and LIA, given the rather sparse and scanty observations for the past climate. Therefore, the fidelity of the historical period simulations (HS; CE 1901–1999) in reproducing the available observations will be our benchmark to decide the suitability of the model simulations for other periods as well, assuming that the responses to the various unit forcings would be analogous.

The HS were generated by forcing the models with the observed atmospheric constituent composition of natural and anthropogenic aerosols (or their precursors), natural sources of short-lived species, time-evolving land cover and solar forcing for the period[101]. The last millennium simulations for the period (MWP and LIA) were generated by forcing with evolving solar and volcanic aerosols, land use changes and well-mixed greenhouse gases[102]. The mid-Holocene simulations were generated with orbital parameters and atmospheric concentrations of well-mixed greenhouse gases for the period[102]. The glacial maximum simulations, for the period, were generated by forcing with orbital parameters, ice sheets and atmospheric concentrations of well-mixed greenhouse gases[102].

The ability of various CMIP5/PMIP3 models, including reproducing observed trends in rainfall and surface temperatures as well as the observed negative correlation between ENSO and ISMR for the historical periods were already reported[36,108]. We briefly revisit the fidelity of the HS with the ERA-20CM skin temperature (SKT)[109], and the India Meteorological Department (IMD) gridded rainfall datasets for the CE 1901–2009 period[16] (available at 1.0° lat. × 1.0° long resolution and covering the Indian land region bound by 66.5°E–101.5°E; 6.5°N–39.5°N). In this study, we start with the validation of the 99-year climatological cycle of the simulated ISMR of the HS with observed ISMR. We mainly concentrate on the seasonal cycle changes, ENSO–ISM teleconnections and 850 hPa large scale circulation (velocity potential) patterns with respect to the HS.

Results and discussion

Figure 1 presents the mean climatological seasonal cycles of the area-averaged surface temperature and rainfall from the CMIP5 HS, along with those from the available

observational datasets. Figure 1 *a* shows that the CCSM4 model is able to capture the observational evolution of climatological SKT; other models show a slight shift. The CCSM4 model captures the observational seasonal evolution of the area-averaged rainfall over India, interestingly, also captures the magnitude reasonably well (Figure 1 *b*). While the other four models can produce the spurt in monsoon season since June (Figure 1 *b*), the simulations, however, indicate a pronounced dry-bias compared to the observations. This is also reflected in the relatively warmer simulated months of June and July compared to the observations (Figure 1 *a*). The correlation coefficients between the area-averaged ISM surface temperatures and rainfall from all the models during HS (vary over a wide range of –0.73 to –0.16) are significantly negative at 0.05 level from Student's 2-tailed test and are in phase with the current-day observational values. In summary, we can use these simulations for further analysis to check the changes in the general climatology of the ISM during the different past climatic periods.

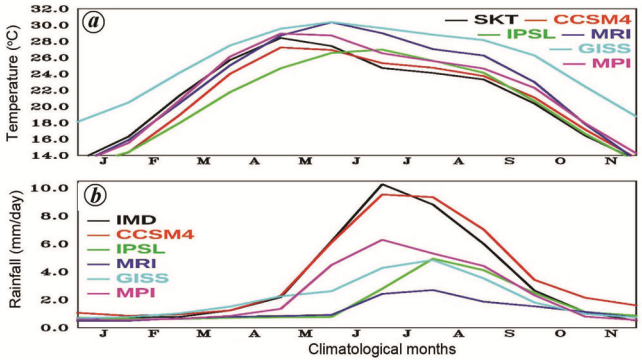

Figure 1. Comparisons of observed and simulated area-averaged climatological cycle for the HS period (CE 1901–1999) for (***a***) surface temperature and (***b***) rainfall over the Indian land region (66.5°E–101.5°E; 6.5°N–39.5°N).

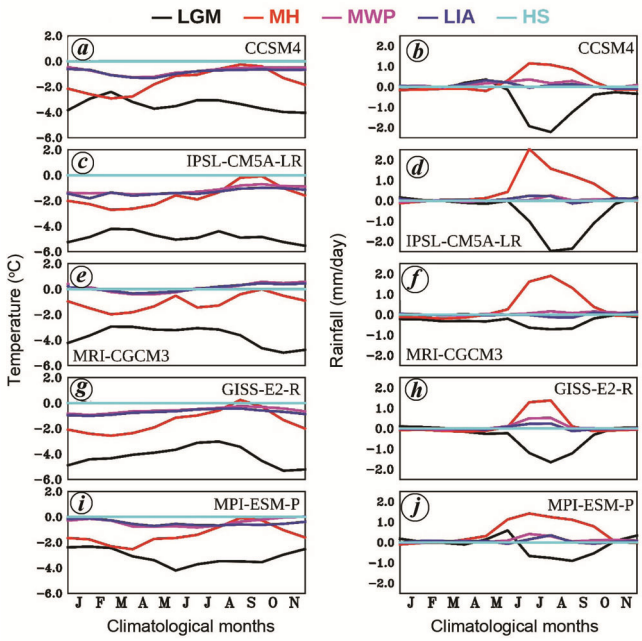

Figure 2. Differences in area-averaged seasonal cycle for each past time slice compared to that for the HS. Panels; (***a***), (***c***), (***e***), (***g***) and (***i***) are for surface temperature of each model over Indian land region; (***b***), (***d***), (***f***), (***h***) and (***j***) are the corresponding differences in simulated rainfall. The descriptor string each panel indicates the name of the model. The HS differences from its own values, naturally zero, are shown in cyan.

Figure 2 compares the differences in the seasonal cycle of surface temperature from each past climate simulation to that from the HS, obtained by the HS signal from the corresponding signal from the past climate simulation. A similar inter-comparison of the simulated seasonal cycle of the area-averaged monthly rainfall across the Indian land region is also presented in Figure 2. It confirms that the models reproduce the expected temperature response to increased greenhouse gases, from the sense that the GHGs have increased in the recent period, and thus reliable. The temperatures in the LGM are found to be coldest across all the models, followed by the MH period (Figure 2 *a*, *c*, *e*, *g* and *i*). Interestingly, the simulated rainfall over India, particularly during the summer monsoon season, is least during the LGM, in agreement with the proxy study by Marzin *et al.*[109]. The simulated summer monsoon rainfall is found to be highest for the MH period. This simulated high Indian summer monsoon rainfall during ~6 kyr BP supports the results from the proxy studies such as Band *et al.*[56] and Rawat *et al.*[64], but in contrast with Dixit *et al.*[48] and Rashid *et al.*[110]. It is worth noting that the model simulations, associated with proxy datasets from the eastern tropical Indian Ocean as well as China[35] suggest an increased frequency of the positive IOD events associated with a strong cross-equatorial summer monsoonal flow into India.

The spatial distributions of the simulated summer monsoon rainfall during various past climate periods relative to HS are presented in Figure 3. All the five models simulate a relatively excess summer monsoon rainfall during MH across the Indian region, and relatively dry summer conditions during the LGM (Figure 3). While the simulations also show, in general, a wetter MWP and LIA summer monsoons over India (Figure 3), it can be seen from Figure 3 that the simulated summer monsoon rainfall during the LIA is substantially less than that for the MWP across all the models.

Figure 4 presents the excess/deficit JJAS 850 hPa velocity potential (χ_{850} $m^2 s^{-1}$) relative to that for the HS. It is evident that the Indian subcontinent was home to large scale low-level divergence during the LGM relative to that for the HS, but a relatively strong convergence during the MH period. These changes in the large-scale circulation during the summer monsoon season in each time slice could be one of the main reasons for the precipitation changes over India[36,37,77].

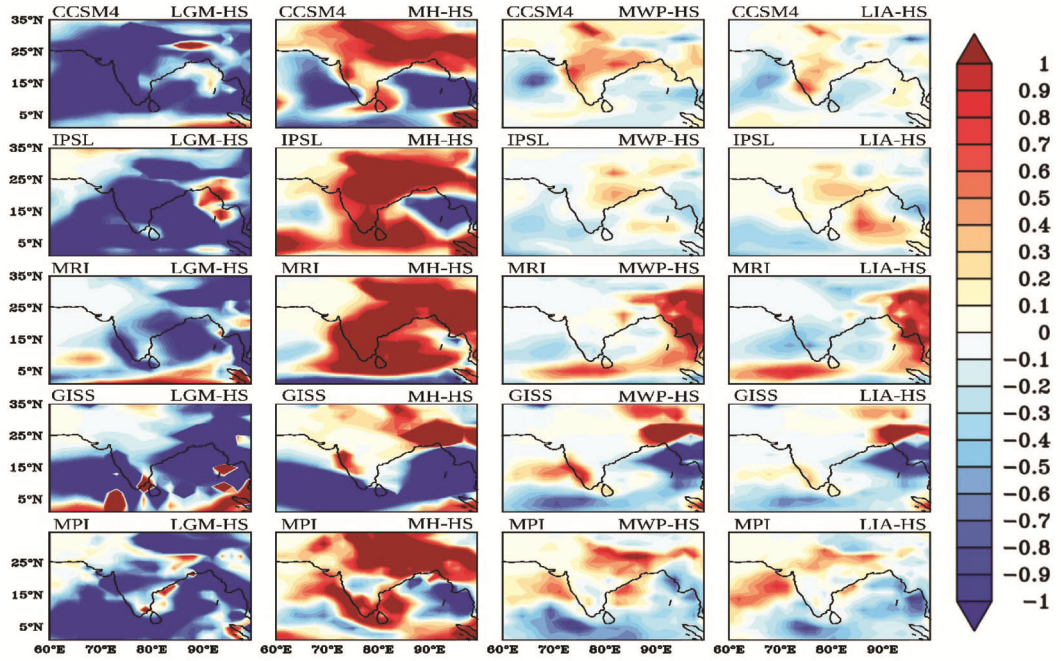

Figure 3. Spatial distributions of the simulated summer monsoon rainfall (mm/day) during various past periods relative to that for the HS. The descriptor string above each panel indicates the name of the model and the periods over which the difference is calculated.

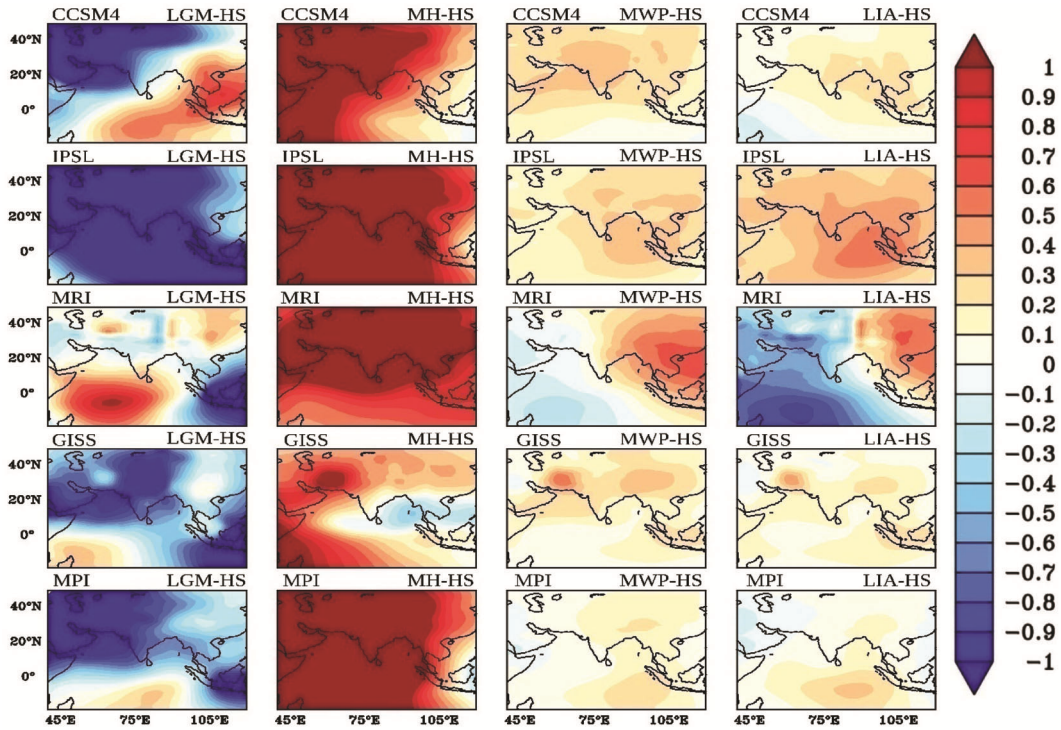

Figure 4. Same as Figure 3, but for the simulated 850 hPa differences in the time-averaged JJAS velocity potential 'χ_{850}' ($m^2\ s^{-1}$).

ENSO being a major climatic driver for the ISM variability, it will be informative to check the ENSO–ISM association in the simulated past climate. We calculated the linear correlations of the NINO 3.4 index with the Indian summer monsoon rainfall, and surface temperatures respectively (Figure 5). It is clearly seen that the ENSO–ISM correlation is negative during the MH, but weaker in magnitude than those of the LGM, MWP and

LIA epochs; all the correlations, however, are significant at 0.05 level from Student's 2-tailed test. Notably, the HS correlations are even weaker than those of the MH. Furthermore, to check the ENSO stability, we show the ENSO variance for all the time slices (Figure 6). Indeed, the simulated ENSO variance by the CCSM4, IPSL-CM5A-LR and MPI-ESM-P models is weakest for the MH. The simulated ENSO variance by the GISS-E2-R model is, however, highest during MH among all the time periods we examined. The MRI-CGCM3 model ENSO variance does not change much in all the time slices.

Providing detailed analysis and dynamics behind the changes in precipitation and surface temperature patterns over the Indian subcontinent during the past climate periods is beyond the scope of this article.

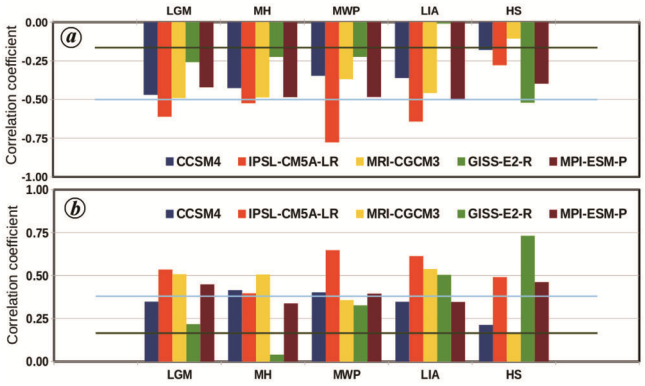

Figure 5. Simulated boreal summer (JJAS) NINO3.4 index correlation coefficients for each time slice and model, for time slices of LGM, MH, MWP, LIA and HS for the models CCSM4 (blue), IPSL-CM5A-LR (red), MRI-CGCM3 (yellow), GISS-E2-R (green) and MPI-ESM-P (brown) between respective time period of simulated NINO3.4 index with (***a***) rainfall (***b***) surface temperatures. Dark green line shows the present day (CE 1901–1999) observational correlation values, and cyan line show the statistical significance at 0.05 level from a 2-tailed Student's *t*-test.

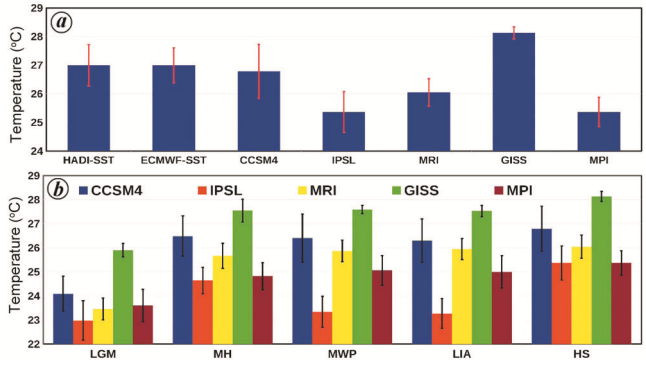

Figure 6. Mean NINO3.4 index and error bars of standard deviation for (***a***) both observations (HadISST, and ECMWF SST) and simulations during the HS period, and (***b***) for the simulated NINO3.4 index for LGM, MH, MWP, LIA and HS. The data for the models CCSM4, IPSL-CM5A-LR, MRI-CGCM3, GISS-E2-R and MPI-ESM-P are shown in blue, red, yellow, green and brown respectively.

Conclusions and scope for future study

The Indian summer monsoon climate variability manifests on interannual to millennial to multi-millennial time scales[47,80]. Proxy-based studies mention that Indian monsoon precipitation was weaker than the present in the LGM period[111], but stronger during early to mid-Holocene period (~12 kyr – 8kyr BP)[53,64,110,111]. The relatively high Indian summer monsoon simulated for the ~6 kyr BP period is in conformation with the inferences from proxy studies by Band *et al.*[56] and Rawat *et al.*[64].

Relevantly, Rehfeld and Laepple[98] report a timescale-based relationship between the temperature and rainfall over the Indian region from their analysis of instrumental and proxy data, specifically, negative correlations on annual to decadal timescales, e.g. cool and wet summers; however, positive correlations are found on longer timescales between precipitation and temperature. Importantly, Rehfeld and Laepple[98] find, in contrast, negative correlations between precipitation and temperature from CMIP5/PMIP3 climate model simulations on all timescales. In this context, based on our analysis of mainly summer monsoon conditions, which is mainly on interannual time scales, we find a cool and dry condition over the Indian region for the LGM in all the models (Figure 2). Indeed, a positive relationship between the responses of the summer monsoon rainfall and temperature is also seen for the MWP and LIA. We have already shown[37] that such a response for the MWP and LIA is not necessarily an artefact, but can be explainable as an interaction between the interannual circulation changes associated with the ENSO with centennial modulations in the Walker circulation. Interestingly, while all the models simulate a wet MH relative to the modern period, the response in the temperature is not so uniform across the models (Figure 2). Nonetheless, as discussed in the previous section, at least the rainfall response seems to be homogeneous across all the model outputs analysed and is supported in general by conclusions from the proxy-observations in the majority of cases. We have to bear in mind that the resolution of the models is rather coarse, and response at local levels need not adhere to that from the area-averaged analysis[37]. Therefore, downscaling of the PMIP3 simulations would be useful to understand the processes of not only the interannual variability better, but also the sensitivity of the rainfall–temperature relationships to the timescales at which such relationships are viewed[99,112].

The simulated variance of the NINO 3.4 index, which is an index of the ENSO activity, shows a decrease during the MH period compared to the other past epoch simulations, and in the HS. The simulated ENSO–ISMR correlation, however, is significant at 0.05 level from Student's 2-tailed test across the past time periods. The changes in the large-scale circulation patterns apparently played a major role in the precipitation changes over the Indian

region. It would be interesting to check whether the changes in large scale monsoon circulation during summer are attributed to the changes in the tropical Indo-pacific characteristics, which themselves may or may not have been modulated by the solar forcing changes[36,37,77].

Furthermore, the assessment of climate changes on millennial time scales requires a consideration of major components of the earth system typically not represented in the IPCC-type simulations (e.g. interactive ice sheets, marine sediments, etc.) To elaborate, for example, the strong sea-level change suggested to have occurred during the early Holocene, is attributed to the ice sheets that were still melting. Understanding the relevance of changes in sea level to the past climate change of monsoons would not be possible using models without an interactive sea ice component. It is pertinent to recall that 'In order to determine the past climate variability of Indian or any other region with better accuracy we have to put our efforts in the synthesis of data model including the comparisons of palaeo simulation outputs and reconstructed palaeoclimate proxy data assimilation[113,114]'.

1. Parthasarathy, B. A., Munot, A. A. and Kothawale, D. R., Regression model for estimation of foodgrain production from summer monsoon rainfall. *Agric. Forest Meteorol.*, 1988, **42**, 167–182.
2. Parthasarathy, B., Rupa Kumar, K. and Munot, A. A., Forecast of rainy-season food grain production based on monsoon rainfall. *Indian J. Agric. Sci.*, 1992, **62**, 1–8.
3. Gadgil, S., Climate change and agriculture – an Indian perspective. In *Climate Variability and Agriculture* (eds Abrol, Y. R., Gadgil, S. and Pant, G. B.), Narosa, New Delhi, India, 1996, pp. 1–18.
4. Webster, P. J., Magana, V. O., Palmer, T. N., Shukla, J., Tomas, R. A., Yanai, M. and Yasunari, T., Monsoons: processes, predictability, and the prospects for prediction. *J. Geophys. Res.*, 1998, **103,** 14,451–14,510.
5. Krishna Kumar, K., Rupa Kumar, K., Raghavendra, A., Nayana, D. and James, H., Climate impacts on Indian agriculture. *Int. J. Climatol.*, 2004, **24**, 1375–1393; 10.1002/joc.1081.
6. Hemadri, A. and Karumuri, A., Relevance of Indian Summer Monsoon and its Tropical Indo-Pacific Climate Drivers for the Kharif Crop Production. *Pure Appl. Geophys.*, 2017, **175**; 10.1007/s00024-017-1758-9.
7. Pattanaik, D. R., *Indian Monsoon Variability*, Meteorological Monograph, 2012, vol. 2, Ch. 2, pp. 35–77.
8. Guhathakurta, P. and Rajeevan, M., Trends in the rainfall pattern over India. *Int. J. Climatol.*, 2008, **28**, 1453–1469; doi: 10.1002/joc.1640.
9. Goswami, B. N., Madhusoodanan, M., Neema, C. and Sengupta, D., A physical mechanism for North Atlantic SST influence on the Indian summer monsoon. *Geophys. Res. Lett.*, 2006, **33**, L02706.
10. Guhatakurtha, P. and Rajeevan, M., Trends in the rainfall pattern over India. National climate centre (NCC). *India Meteorol. Dept. Res. Rep.*, 2006, **2**, 1–23.
11. Krishnan, R. *et al.*, Will the South Asian monsoon overturning circulation stabilize any further? *Clim. Dyn.*, 2012, **40**, 187–211.
12. Sanap, S. D., Pandithurai, G. and Manoj, M. G., On the response of Indian summer monsoon to aerosol forcing in CMIP5 model simulations. *Clim. Dyn.*, 2015; doi:10.1007/s00382-015-2516-2.
13. Krishnan, R., Sabin, T. P. and Vellore, R., Deciphering the desiccation trend of the South Asian monsoon hydroclimate in a warming world. *Clim. Dyn.*, 2016, **47**, 1007; https://doi.org/10.1007/s00382-015-2886-5.
14. Roxy, M. K., Ritika, K., Terray, P., Murtugudde, R., Ashok, K. and Gowswami, B. N., Drying of Indian subcontinent by rapid Indian Ocean warming and a weakening land–sea thermal gradient. *Nature Commun.*, 2015.
15. Ross Robert, S., Krishnamurti, T. N., Sandeep, P. and Pai, D. S., Decadal surface temperature trends in India based on a new high-resolution data set. *Sci. Rep.*, 2018, **8**, 7452; doi:10.1038/s41598-018-25347-2.
16. Rajeevan, M., Bhate, J., Kale, J. D. and Lal, B., High resolution daily gridded rainfall data for the Indian region? *Anal. Break Active Monsoon Spells*, 2006, **91**(3).
17. Pai, D. S., Sridhar, L., Rajeevan, M., Sreejith, O. P., Satbhai, N. S. and Mukhopadhyay, B., Development of a new high spatial resolution (0.25° × 0.25°) long period (1901–2010) daily gridded rainfall data set over India and its comparison with existing data sets over the region. *Mausam*, 2014, **65**(1), 1–18.
18. Kothawale, D. R. and Singh, H. N., Recent trends in tropospheric temperature over India during the period 1971–2015. *Earth Space Sci.*, 2017, **4**, 240–246; doi:10.1002/2016EA000246.
19. Walker, G. T., Correlation in seasonal variation of weather. *Q. J. R. Meteorol. Soc.*, 1918, **44**, 223–234.
20. Blandford, H. F., On the connexion of the Himalayan snowfall with dry winds and seasons of drought in India. *Proc. R. Soc. London*, 1884, **37**, 1–23.
21. Kumar, K. K., Rajagopalan, B. and Cane, M. A., On the weakening relationship between the Indian Monsoon and ENSO. *Science*, 1999, **284**(5423), 2156–2159.
22. Saji, N. H., Goswami, B. N., Vinayachandran, P. N. and Yamagata, T., A dipole mode in the tropical Indian Ocean. *Nature*, 1999, **401**, 360–363.
23. Webster, P. J., Moore, A., Loschnigg, J. and Leban, M., Coupled dynamics in the Indian Ocean during 1997–1998. *Nature*, 1999, **401**, 356–360.
24. Murtugudde, R., McCreary, J. P. and Busalacchi, A. J., Oceanic processes associated with anomalous events in the Indian Ocean with relevance to 1997–1998. *J. Geophys. Res.*, 2000, **105**, 3295–3306.
25. Ashok, K., Guan, Z. and Yamagata, T., Impact of the Indian Ocean dipole on the relationship between the Indian monsoon rainfall and ENSO. *Geophys. Res. Lett.*, 2001, **28**(23), 4499–4502.
26. Ashok, K., Guan, Z., Saji, N. H. and Yamagata, T., Individual and combined influences of ENSO and the Indian Ocean dipole on the Indian summer monsoon. *J. Climate*, 2004, **17**(16), 3141–3155.
27. Kripalani, R. H. and Kulkarni, A., Climatological impact of El Niño/La Niña on the Indian monsoon: a new perspective. *Weather*, 1999, **52**, 39–46.
28. Krishnamurthy, V. and Goswami, B. N., Indian monsoon-ENSO relationship on inter decadal time scales. *J. Climate*, 2000, **13**, 579–595.
29. Krishnan, R. and Sugi, M., Pacific decadal oscillation and variability of the Indian summer monsoon rainfall. *Clim. Dyn.*, 2003, **21**, 233–242.
30. Krishnamurthy, L. and Krishnamurthy, V., Influence of PDO on South Asian summer monsoon and monsoon-ENSO relation. *Clim. Dyn.*, 2014, **42**, 2397–2410.
31. Feba, F., Ashok, K. and Ravichandran, M., Role of changed Indo-Pacific atmospheric circulation in the recent disconnect between the Indian summer monsoon and ENSO. *Clim. Dyn.*, 2018; https //doi.org/10.1007/s00382-018-4207-2.
32. Gershunov, A., Schneider, N. and Barnett, T., Low-frequency modulation of the ENSO-Indian monsoon rainfall relationship: signal or noise? *J. Climate*, 2001, **14**, 2486–2492.

33. Ashok, K. and Saji, N. H., Impacts of ENSO and Indian Ocean dipole events on the sub-regional Indian Summer Monsoon rainfall. *J. Natural Hazards*, 2007, **42**, 273–285.
34. Ashok, K., Feba, F. and Tejavath, C. T., The Indian summer monsoon rainfall and ENSO. *Mausam*, 2019, **70**, 443–452.
35. Abram, N. J., Michael, K., Gagan, Zhengyu Liu, Wahyoe, S., Hantoro, McCulloch, M. T. and Suwargadi, B. W., Seasonal characteristics of the Indian Ocean Dipole during the Holocene epoch. *Nature*, 2007, **445**, doi:10.1038/nature05477.
36. Tejavath, C. T., Karumuri, A., Chakraborty, S. and Ramesh, R., The Indian summer monsoon climate during the Last Millennium, as simulated by the PMIP3. *Clim. Past Discuss*, 2017; https://doi.org/10.5194/cp-2017-24.
37. Tejavath, C. T., Karumuri, A., Chakraborty, S. and Ramesh, R., A PMIP3 narrative of modulation of ENSO teleconnections to the Indian summer monsoon by background changes in the Last Millennium. *Climate Dyn.*, 2019; https://doi.org/10.1007/s00382-019-04718-z.
38. An, S.-I. and Choi, J., Mid-Holocene tropical Pacific climate state, annual cycle, and ENSO in PMIP2 and PMIP3. *Clim. Dyn.*, 2013, **43**, 957–970; doi:https://doi.org/10.1007/s00382-013-1880-z.
39. Chabangborn, A., Brandefelt, J. and Wohlfarth, B., Asian monsoon climate during the Last Glacial Maximum: palaeo-data–model comparisons. *Boreas*, 2013; 10.1111/bor.12032. ISSN 0300-9483.
40. Raza, W., Ahmad, S. M. and Lone, M. A., Indian summer monsoon variability in southern India during the last deglaciation: Evidence from a high resolution stalagmite δ^{18}O record. *Palaeogeogr., Palaeoclimatol., Palaeoecol.*, 2017, **485**, 476–485.
41. Ali, S. N. *et al.*, High frequency abrupt shifts in the Indian summer monsoon since Younger Dryas in the Himalaya. *Sci. Rep.*, 2018, **8**(1), 9287.
42. Sandeep, K., Shankar, R., Warrier, A. K., Yadava, M. G., Ramesh, R., Jani, R. A., Weijian, Z. and Xuefeng, L., A multi-proxy lake sediment record of Indian summer monsoon variability during the Holocene in southern India. *Palaeogeogr., Palaeoclimatol., Palaeoecol.*, 2017, **476**, 1–14.
43. Steinhilber, F., Beer, J. and Frölich, C., Total solar irradiance during the Holocene. *Geophys. Res. Lett.*, 2009, **36**, L19704; doi:10.1029/2009GL040142.
44. Mayewski Paul, A. and Coauthors, Holocene climate variability. *Quatern. Res.*, 2004, **62**(3), 243–255; ISSN 0033-5894, https://doi.org/10.1016/j.yqres.2004.07.001.
45. Sarkar, A., Ramesh, R., Somayajulu, B. L. K., Agnihotri, R., Jull, A. J. T. and Burr, O. S., High resolution Holocene monsoon record from the eastern Arabian Sea. *Earth Planet. Sci. Lett.*, 2000, **177**(3–4), 209–218; doi:10.1016/S0012-821X(00)00053-4.
46. Fleitmann, D. *et al.*, Holocene ITCZ and Indian monsoon dynamics recorded in stalagmites from Oman and Yemen (Socotra). *Quat. Sci. Rev.*, 2007, **26**, 170–188.
47. Ramesh, R. *et al.*, Retrieval of south Asian monsoon variation during the holocene from natural climate archives. *Curr. Sci.*, 2010, **99**(12), 1770–1786.
48. Dixit, Y., Hodell, D. A., Sinha, R. and Petrie, C. A., Abrupt weakening of the Indian summer monsoon at 8.2 kyr BP. *Earth Planet. Sci. Lett.*, 2014, **391**, 16–23.
49. Dutt, S., Gupta, A. K., Clemens, S. C., Cheng, H., Singh, R. K., Kathayat, G. and Edwards, R. L., Abrupt changes in Indian summer monsoon strength during 33,800 to 5500 years BP. *Geophys. Res. Lett.*, 2015, **42**, 5526–5532.
50. Nakamura, A. *et al.*, Weak monsoon event at 4.2 ka recorded in sediment from Lake Rara, Himalayas. *Quat. Int.*, 2015; http://dx.doi.org/10.1016/j.quaint.2015.05.053.
51. Gill, E. C., Rajagopalan, B., Molnar, P. H., Kushnir, Y. and Marchitto, T. M., Reconstruction of Indian summer monsoon winds and precipitation over the past 10,000 years using equatorial pacific SST proxy records, *Paleoceanography*, 2017, **32**, 195–216; doi:10.1002/2016PA002971.
52. Prasad, S. *et al.*, Prolonged monsoon droughts and links to Indo-Pacific warm pool: a Holocene record from Lonar Lake, Central India. *Earth Planet. Sci. Lett.*, 2014, **391**, 171–182.
53. Dixit, Y., Hodell, D. A. and Petrie, C. A., Abrupt weakening of the summer monsoon in northwest India ~4100 year ago. *Geology*, 2014, **42**, 339–342.
54. Yuan, D. *et al.*, Timing, duration, and transitions of the Last Interglacial Asian monsoon. *Science*, 2004, **304**, 575–578.
55. Pausata, F. S. R. *et al.*, Greening of the Sahara suppressed ENSO activity during the mid-Holocene. *Nat. Commun.*, 2017, **8**, 16020; doi:10.1038/ncomms16020.
56. Band, S., Yadava, M. G., Mahjoor, A. L., Chuan-Chou, S., Kaushik, S. and Ramesh, R., High-resolution mid-Holocene Indian Summer Monsoon recorded in a stalagmite from the Kotumsar Cave, Central India. *Quat. Int.*, 2018, 479.
57. Jalihal, C., Bosmans, J. H. C., Srinivasan, J. and Chakraborty, A., The response of tropical precipitation to Earth's precession: the role of energy fluxes and vertical stability. *Clim. Past*, 2019, **15**, 449–462; https://doi.org/10.5194/cp-15-449-2019.
58. Sharma, S. and Anil, D. Shukla, Factors governing the pattern of glacier advances since the Last Glacial Maxima in the transitional climate zone of the Southern Zanskar Ranges, NW Himalaya. *Quat. Sci. Rev.*, 2018, 201.
59. Staubwasser, M., Sirocko, F., Grootes, P. M. and Segl, M., Climate change at the 4.2 ka BP termination of the Indus valley civilization and Holocene south Asian monsoon variability. *Geophys. Res. Lett.*, 2003, **30**, 1425; http://dx.doi.org/10.1029/2002GL016822.
60. Dixit, Y. *et al.*, Intensified summer monsoon and the urbanization of Indus Civilization in northwest India. *Sci. Rep.*, 2018, **8**, 4225; https://doi.org/10.1038/s41598-018-22504-5.
61. Dutt, *et al.*, A long arid interlude in the Indian summer monsoon during ~4,350 to 3,450 cal. yr BP contemporaneous to displacement of the Indus valley civilization. *Quat. Int.*, 2018, **482**, 83–92.
62. Berkelhammer, M., Sinha, A., Stott, L., Cheng, H., Pausata, Francesco, S. R. and Yoshimura, K., An abrupt shift in the Indian Monsoon 4000 years ago, chapter in Geophysical Monograph Series: Climate Landscapes and Civilization, 2012; doi:10.1029/2012GM001207.
63. Giosan Liviu *et al.*, Fluvial landscapes of the Harappan civilization. *Proc. Natl. Acad. Sci.*, 2012, **109**(26), E1688–E1694; doi:10.1073/pnas.1112743109.
64. Rawat, S., Gupta, A. K., Sangode, S. J., Srivastava, P. and Nainwal, H. C., Late Pleistocene–Holocene vegetation and Indian summer monsoon record from the Lahaul, Northwest Himalaya, India. *Quat. Sci. Rev.*, 2015, **114**, 167–181.
65. Sinha, N., Gandhi, N., Chakraborty, S., Krishnan, R., Yadava, M. and Ramesh, R., Abrupt climate change at ~2800 year BP evidenced by a stalagmite record from peninsular India. *The Holocene*, 2018, **28**(11), 1720–1730; https://doi.org/10.1177/0959683618788647.
66. Gill, E. C., Rajagopalan, B., Molnar, P. and Marchitto, T. M., Reduced-dimension reconstruction of the equatorial Pacific SST and zonal wind fields over the past 10,000 years using Mg/Ca and alkenone records. *Paleoceanography*, 2016, **31**, 928–952; doi:10.1002/2016PA002948.
67. Moy, C. M., Seltzer, G. O., Rodbell, D. T. and Anderson, D. M., Variability of El Nino/Southern Oscillation activity at millennial timescales during the Holocene epoch. *Nature*, 2002, **420**, 162–165.
68. Gagan, M. K., Hendy, E. J., Haberle, S. G. and Hantoro, W. S., Post-glacial evolution of the Indo-Pacific Warm Pool and El Nino-Southern Oscillation. *Quat. Int.*, 2004, 118–119, 127–143.
69. Lu Zhengyao, Zhengyu Liu, Jiang Zhu and Kim M. Cobb A Review of Paleo El Niño-Southern Oscillation. *Atmosphere*, 2018, **9**, 130; doi:10.3390/atmos9040130.

70. Steven, P. J. and Brown, J. N., Understanding ENSO dynamics through the exploration of past climates. *IOP Conf. Series: Earth Environ. Sci.*, 2010, **9**, 012010; doi:10.1088/1755-1315/9/1/012010.
71. Dixit, Y. and Tandon, S. K., Earth-science reviews hydroclimatic variability on the Indian subcontinent in the past millennium? Review and assessment. *Earth Sci. Rev.*, 2016, **161**, 1–15; http://doi.org/10.1016/j.earscirev.2016.08.001.
72. Cook, E. R., Anchukaitis, K. J., Buckley, B. M., D'Arrigo, R. D., Jacoby, G. C. and Wright, W. E., Asian monsoon failure and megadrought during the last millennium. *Science*, 2010, **328**, 486–489.
73. Rehfeld, K., Marwan, N., Breitenbach, S. F. M. and Kurths, J., Late Holocene Asian summer monsoon dynamics from small but complex networks of paleoclimate data. *Clim. Dyn.*, 2013, **41**, 3–19.
74. Overpeck, J. T., Anderson, D. M., Trumbore, S. and Prell, W. L., The southwest Indian monsoon over the last 18,000 years. *Clim. Dyn.*, 1996, **12**, 213–225; https://doi.org/10.1007/BF00211619.
75. Sinha, A. *et al.*, A 900-year (600 to 1500 AD) record of the Indian summer monsoon precipitation from the core-monsoon zone of India. *Geophys. Res. Lett.*, 2007, **34**.
76. Sanwal *et al.*, Climatic variability in Central Indian Himalaya during the last ~1800 years: evidence from a high resolution speleothem record. *Quat. Int.*, 2013, **304**, 183–192.
77. Polanski, S., Bijan Fallah, Daniel J. Befort, Sushma Prasad and Ulrich Cubasch, Regional moisture change over India during the past Millennium: a comparison of multi-proxy reconstructions and climate model simulations. *Global Planet. Change*, 2014, **122**, 176–185.
78. Polanski, S., Fallah, B., Prasad, S. and Cubasch, U., Simulation of the Indian monsoon and its variability during the last millennium, *Clim. Past Discuss.*, 2013, **9**, 703–740; doi:10.5194/cpd-9-703-2013.
79. Ummenhofer, C., Caroline, Rosanne D. D'Arrigo, Kevin J. Anchukaitis, Brendan M. Buckley, Edward R. Cook, Links between Indo-Pacific climate variability and drought in the Monsoon Asia Drought Atlas. *Clim. Dyn.*, 2013, **40**, 1319–1334; doi:10.1007/s00382-012-1458-1.
80. Chakraborty, S., Goswami, B. N. and Dutta, K., Pacific coral oxygen isotope and the tropospheric temperature gradient over Asian monsoon region: a tool to reconstruct past Indian summer monsoon rainfall. *J. Quat. Sci.*, 2012, **27**(3) 269–278; doi:10.1002/jqs.1541.
81. Sinha, A., Gayatri Kathayat, H., Cheng, Sebastian, F. M., Breitenbach, M., Berkelhammer, M. and Mudelsee, J., Trends and oscillations in the Indian summer monsoon rainfall over the last two millennia. *Nat. Commun.*, 2015; https://doi.org/10.1038/ncomms7309
82. Liu, Z., Otto-Bliesner, B., Kutzbach, J., Li, L. and Shields, C., Coupled climate simulation of the evolution of global monsoons in the Holocene. *J. Clim.*, 2003, **16**(15), 2472–2490.
83. Bosmans, J., Drijfhout, S., Tuenter, E., Lourens, L., Hilgen, F. and Weber, S., Monsoonal response to mid-Holocene orbital forcing in a high resolution GCM. *Clim. Past*, 2012, **8**, 723–740.
84. Braconnot, P. *et al.*, Results of PMIP2 coupled simulations of the mid-Holocene and last glacial maximum. Part 1: experiments and large-scale features. *Clim. Past*, 2007, **3**(2), 261–277.
85. Braconnot, P. *et al.*, Results of PMIP2 coupled simulations of the mid-Holocene and last glacial maximum. Part 2: feedbacks with emphasis on the location of the ITCZ and mid- and high latitudes heat budget. *Clim. Past*, 2007, **3**(2), 279–296.
86. Marzin, C. and Braconnot, P., Variations of Indian and African monsoons induced by insolation changes at 6 and 9.5 kyr BP, *Clim. Dyn.*, 2009, **33**(2–3), 215–231.
87. Zheng, W., Braconnot, P., Guilyardi, E., Merkel, U. and Yu, Y., ENSO at 6 ka and 21 ka from ocean-atmosphere coupled model simulations. *Clim. Dyn.*, 2008, **30**(7–8), 745–762.
88. Zhao, Y. *et al.*, A multi-model analysis of the role of the ocean on the African and Indian monsoon during the mid-Holocene. *Clim. Dyn.*, 2005, **25**(7–8), 777–800.
89. Kumar, P., Sanwal, J., Dimri, A. P. and Ramesh, R., Contribution of diverse monsoon precipitation over Central and Northern India during Mid to Late Holocene. *Quat. Int.*, 2019, **507**, 217–223.
90. Gadgil, S., Part 4. Links to cloud systems over the tropical Oceans. *Resonance*, 2008, **13**(3), 218–235.
91. Polanski, S., Rinke, A., Dethloff, K., Lorenz, S. J., Wang, Y. and Herzschuh, U., Simulation of the mid-Holocene Indian summer monsoon circulation with a regional climate model. *Open Atmos. Sci. J.*, 2012, **6**, 42–48.
92. Kitoh, A., Variability of Indian monsoon-ENSO relationship in a 1000-year MRI-CGCM2.2 simulation. *Natural Haz.*, 2007, **42**(2), 261–272; http://doi.org/10.1007/s11069-006-9092-z.
93. Fallah, B. and Cubasch, U., A comparison of model simulations of Asian mega-droughts during the past millennium with proxy reconstructions. *Clim. Past Discuss*, 2014, **10**, 2685–2716.
94. Singh, D. S., Gupta, A. K., Sangode, S. J., Clemens, S. C., Prakasam, M., Srivastava, P. and Prajapati, S. K., Multiproxy record of monsoon variability from the Ganga Plain during 400–1200 AD. *Quat. Int.*, 2015, **371**, 157–163.
95. Carre, M. *et al.*, Holocene history of ENSO variance and asymmetry in the eastern tropical Pacific. *Science*, 2014, **345**, 1045–1048; doi:10.1126/science.1252220.
96. Atwood, A. R., Wu, E., Frierson, D. M. W., Battisti, D. S. and Sachs, J. P., Quantifying climate forcings and feedbacks over the last millennium in the CMIP5–PMIP3 models. *J. Clim.*, 2015, **29**, 1161–1178; doi:10.1175/JCLI-D-15-0063.1.
97. Bond, G. *et al.*, Persistent solar influence on north Atlantic climate during the Holocene. *Science*, 2001, **294**, 2130–2136; doi:10.1126/science.1065680.
98. Rehfeld, K. and Laepple, T., Warmer and wetter or warmer and dryer? Observed versus simulated covariability of Holocene temperature and rainfall in Asia. *Earth Planet. Sci. Lett.*, 2016, **436**, 1–9; doi:10.1016/j.epsl.2015.12.02.
99. Braconnot, P. and Kageyama, M., Shortwave forcing and feedbacks in last glacial maximum and mid-Holocene PMIP3 simulations. *Philos. Trans. R. Soc. A*, 2015, **373**, 20140424; http://dx.doi.org/10.1098/rsta.2014.0424.
100. Braconnot, P., Marti, O. and Joussaume, S., Adjustment and feedbacks in a global coupled ocean-atmosphere model. *Clim. Dyn.*, 1997, **13**, 507–519.
101. Taylor, K. E., Stouffer, R. J. and Meehl, G. A., An overview of CMIP5 and the experiment design. *Am. Meteor. Soc. B*, 2012, **93**, 485–498; doi:10.1175/BAMS-D-11-00094.1.
102. Schmidt, G. A. *et al.*, Climate forcing reconstructions for use in PMIP simulations of the Last Millennium (v1.1). *Geosci. Model Dev.*, 2012, **5**, 185–191; doi:10.5194/gmd- 5-185-2012.
103. Stocker, T. F. *et al.*, Technical Summary. In Climate Change 2013: The Physical Science Basis. Contribution of Working Group I to the Fifth Assessment Report of the Intergovernmental Panel on Climate Change. Cambridge University Press, Cambridge, United Kingdom and New York, USA, 2013, pp. 33–115; doi:10.1017/ CBO9781107415324.005.
104. Lamb, H. H., The early medieval warm epoch and its sequel. *Palaeogeogr., Palaeoclimatol.*, 1965, **1**, 13–37.
105. Grove, J. M., *The Little Ice Age*, Menthuen, London, 1988.
106. Graham, N. E., Ammann, C. M., Fleitmann, D., Cobb, K. M. and Luterbacher, J., Support for global climate reorganization during the Medieval Climate Anomaly. *Clim. Dyn.*, 2010, **37**, 1217–1245.
107. Mann, M. E., Zhihua Zhang, Scott Rutherford, Raymond S. Bradley, Malcolm K. Hughes, Drew Shindell, Caspar A., Global signatures and dynamical origins of the little ice age and medieval climate anomaly. *Science*, 2009, **326**(5957), 1256–1260; doi:10.1126/science.1177303.

108. Nicolas, J. C., Gupta, A. S., Taschetto, A. S., Ummenhofer, C. C., Moise, A. F. and Ashok, K., The Indo-Australian monsoon and its relationship to ENSO and IOD in reanalysis data and the CMIP3/CMIP5 simulations. *Clim. Dyn*., 2013, **41**, 3073–3102; doi:10.1007/s00382-013-1676-1.
109. Hersbach, H., ERA-20CM: a twentieth-century atmospheric model ensemble, 2015, 2350–2375; http://doi.org/10.1002/qj.2528.
110. Marzin, C., Braconnot, P. and Kageyama, M., Relative impacts of insolation changes, meltwater fluxes and ice sheets on African and Asian monsoons during the Holocene. *Clim. Dyn*., 2013, **41**; 10.1007/s00382-013-1948-9.
111. Rashid, H., England, H., Thompson, E. and Polyak, L., Late glacial to Holocene Indian Summer Monsoon variability from the Bay of Bengal sediment records. *Terrestrial Atmos. Oceanic Sci*., 2011, **22**, 215–228.
112. Kaushal, N. *et al.*, The Indian Summer Monsoon from a Speleothem δ^{18}O perspective – a review. *Quaternary*, 2018, **1**, 29.
113. Von Storch, H., Langenberg, H. and Feser, F., A spectral nudging technique for dynamical downscaling purposes. *Monthly Weather Rev*., 2000, **128**, 3664–3673; 10.1175/1520-0493(2000)128<3664:ASNTFD>2.0.CO;2.
114. Fang, M. and Li, X, Paleoclimate data assimilation: its motivation, progress and prospects. *Sci. China Earth Sci.*, 2016, **59**, 1817–1826; doi:10.1007/s11430-015-5432-6.

ACKNOWLEDGMENTS. K.A. acknowledges the DST, Government of India, for the Grant DST/19/1901/2017/01061. The CMIP5 and PMIP3 datasets have been downloaded and available from CMIP5 archives e.g. https://cera-www.dkrz.de/WDCC/ui/cerasearch/ and https://esgf-index1.ceda.ac.uk/projects/esgf-ceda/. We acknowledge the guidance and collaboration from Late Prof. R. Ramesh for his support in our earlier work. Useful comments from two anonymous reviewers are gratefully acknowledged. The GrADS (COLA), Ferret (NOAA), NCL (NCAR) and CDO (MPI) tools have been used in this study.

doi: 10.18520/cs/v119/i2/316-327